JOURNAL OF CATALYSIS 131, 260–275 (1991)

# The Formation of Titanium Oxide Monolayer Coatings on Silica Surfaces

S. SRINIVASAN,* A. K. DATYE,* M. HAMPDEN-SMITH,† I. E. WACHS,‡ G. DEO,‡ J. M. JEHNG,‡ A. M. TUREK,‡ AND C. H. F. PEDEN§

*Center for Microengineered Ceramics and Departments of *Chemical and Nuclear Engineering, and †Chemistry, University of New Mexico, Albuquerque, New Mexico 87131; ‡Zettlemoyer Center for Surface Studies and Department of Chemical Engineering, Lehigh University, Bethlehem, Pennsylvania 18015; §Sandia National Laboratories Division 1846, P.O. Box 5800, Albuquerque, New Mexico 87185*

Received February 25, 1991; revised April 19, 1991

The formation of a dispersed titanium oxide layer on Cabosil-fumed silica and on nonporous silica spheres was studied by infrared and Raman spectroscopies and by transmission electron microscopy (TEM). The procedure for obtaining the titania coatings involved reacting the silanol groups on the silica surface with titanium alkoxides under a $N_2$ atmosphere. This self-limiting reaction led to a coating of dispersed titania on the silica spheres with a weight loading between 0.5 and $1.4 \times 10^{-3}$ g/m$^2$. The dispersed titanium oxide on the silica spheres was visible as a surface texturing of the silica in TEM images, and led to over two orders of magnitude increase in the reactivity of the silica spheres for 1-propanol dehydration. Raman spectroscopy and TEM confirmed that the dispersed titania was stable to calcination in dry air at 973 K or to heating under a vacuum of $2 \times 10^{-7}$ Torr up to 1058 K. However, under alcohol dehydration reaction conditions, the dispersed titania transformed into crystals of anatase, 3 nm in diameter. On Cabosil-fumed silica, on the other hand, a similar preparation resulted in a titania loading (per square meter) that was only 7% of that seen on the silica spheres. Higher loadings caused the appearance of bands due to crystalline $TiO_2$ (anatase) in the Raman spectra. The lower monolayer capacity on Cabosil silica can be correlated with the presence of singly bound hydroxyls as seen by IR. The Stober spheres on the other hand show hydroxyl bands that show significant hydrogen bonding. 

## INTRODUCTION

There is growing interest in synthesis of dispersed transition metal oxides as novel catalytic materials (*1*). The catalytic behavior of a dispersed oxide is often remarkably different from that of the bulk oxide. Examples of such behavior are the observed selectivity of dispersed vanadia on titania in selective catalytic reduction of nitric oxide with ammonia (*2*) or in the generation of strong acid sites in systems such as $WO_3/Al_2O_3$ (*3*). The structures of these dispersed oxides have been characterized by techniques such as Raman spectroscopy (*4*), EXAFS (*5*), and selective chemisorption (*6*) and the reactivity of the active sites has been probed by the use of model catalytic reactions. In studies of dispersed oxides, it is often important to know if the oxide is present as a dispersed phase or whether it has aggregated into crystals. At low loadings, the small size of these crystals causes significant line broadening in X-ray diffraction (XRD) powder patterns. Hence, the absence of lines from the crystalline phase in an XRD pattern does not necessarily rule out the presence of small particles of the crystalline oxide. While high-resolution transmission electron microscopy (TEM) can be used for the detection of particles smaller than 1 nm, the contrast from the support often makes unambiguous detection difficult (*7*). The problem becomes especially acute when the dispersed phase is present as a two-dimensional overlayer and the contrast is insufficient to distinguish the dispersed phase from the supporting oxide. Hence, in previous studies of dispersed oxides, TEM has been used most often only



0021-9517/91 $3.00

to determine if the dispersed phase formed crystalline islands of oxide (*8*). The sensitivity for detection of a crystalline phase embedded in an amorphous matrix (such as $TiO_2$ in $SiO_2$) can be improved considerably by image processing techniques as proposed by Sattler and O'Keefe (*9*). In this paper we show that by using nonporous oxide particles as a substrate, it is possible to observe, by TEM, the presence of dispersed metal oxides even before the oxide coalesces into islands of a crystalline phase. Furthermore, knowledge of the surface/volume ratio in this simple geometry support makes it possible to relate the elemental analysis from energy dispersive spectroscopy to derive the surface coverage of the dispersed phase.

Previous studies of dispersed $TiO_2$ on silica (*8*) showed that crystalline $TiO_2$ was formed after calcination at 823 K in dry air. Based on laser Raman spectroscopy, the crystalline phase was identified as $TiO_2$(B) at low loadings (<10 wt%) and $TiO_2$ (anatase) at higher weight loadings. If a titania monolayer is assumed to have a thickness of 0.352 nm [the interlayer spacing for the (101) plane of $TiO_2$ (anatase)], then its density would be $1.37 \times 10^{-3}$ g/m$^2$. Since the surface area of Cabosil silica (EH-5) used in the previous study (*8*) was 300 m$^2$/gm, a monolayer of crystalline $TiO_2$ would correspond to ≈29 wt% $TiO_2$. The formation of crystalline $TiO_2$ at loadings much less than the monolayer capacity expected from the BET surface area implies that the silica surface was unable to stabilize the dispersed metal oxide, a behavior that is in contrast to other supports such as alumina where monolayer dispersions of transition metal oxides have been reported (*3, 10, 11*). In other work in the literature, near-monolayer dispersion of titania has been reported on silica (*12, 13*). McDaniel *et al.* (*12*) found that when a silica was impregnated with an alcohol solution of $Ti(OR)_4$, saturation occurred at about 3.0 Ti/nm$^2$. This would correspond to $3.98 \times 10^{-4}$ g $TiO_2$/m$^2$ which is 30% of the monolayer density. However, Vogt *et al.* (*13*) obtained a titania loading of 24 wt% on a silica having a surface area of 240 m$^2$/gm. In this instance, the titania was deposited by contacting an acidic solution of $TiCl_3$ with the silica, and controlled addition of NaOH to a pH of 8. The differences in the ability of silica to stabilize monolayer dispersions of titania in these previous studies (*8, 12, 13*) may be due to the specific precursors used in prior work, and the possible influence of alkali in modifying the silica surface and stabilizing the deposited titania. Furthermore, in view of the difficulty of detecting crystalline titania by XRD, it would be better to ascertain the monolayer capacity of silica using laser Raman spectroscopy.

To explore this aspect further, we have used Raman spectroscopy in conjunction with IR spectroscopy, TEM, and catalytic measurements to study the state of titania dispersed on silica. We have contrasted the behavior of Cabosil-fumed silica with that of nonporous "Stober" silica spheres which are prepared by hydrolysis of tetraethylorthosilicate (TEOS) under basic conditions (*14*). Titania was used to probe the concentration of surface hydroxyl groups by reacting surface silanols with titanium alkoxide compounds followed by calcination to yield the dispersed oxide.

## EXPERIMENTAL

The model silica support used for this study contained nonporous spherical particles of silica prepared by the method of Stober and Fink (*14*). The Stober spheres were dried in air at 383 K for 2 h to remove any adsorbed molecular water. In a typical experiment, 0.5 g of 270-nm silica spheres were added to a solution of Titanium (IV) tert-butoxide (0.4 g; 1.2 mmol) in THF under a dry nitrogen atmosphere. The suspension was stirred for 0.25 h and filtered under nitrogen on a medium porosity frit. The white solid was washed with three 5-ml portions of THF and then dried *in vacuo*. The experiments on fumed silica used Cabosil silica grade HS-5 (*15*) having a BET surface area of 300 m$^2$/gm. The procedure used to deposit titania on the fumed silica was similar to that

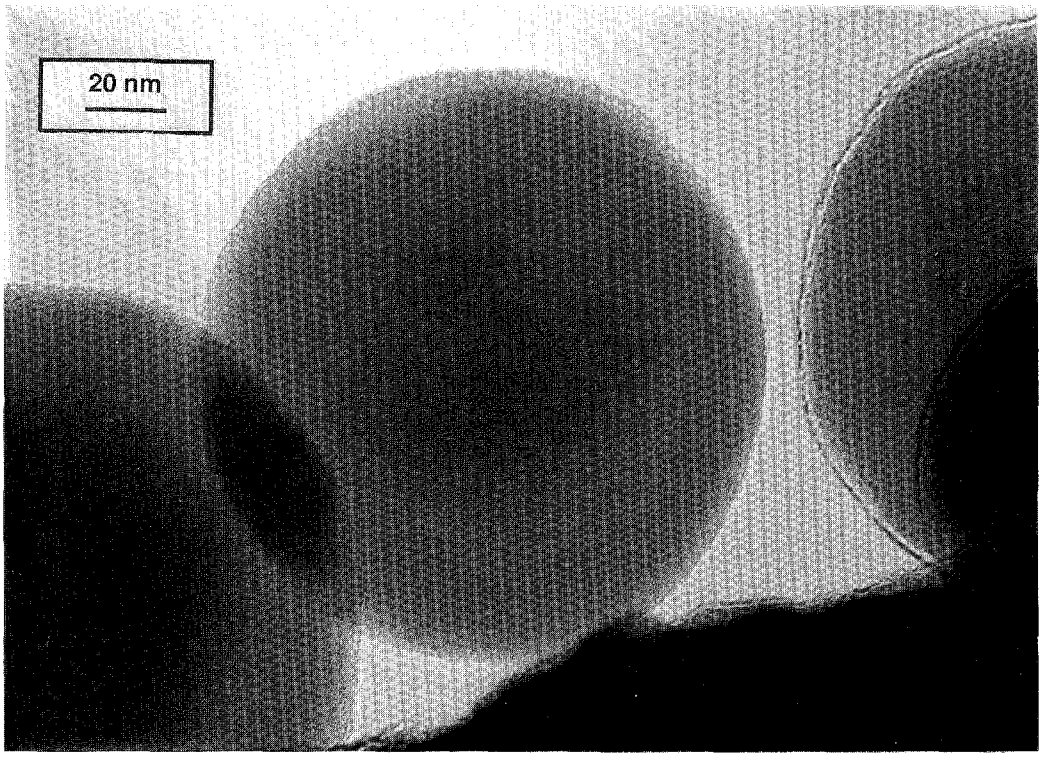


FIG. 1. Electron micrograph of uncoated silica spheres having an average diameter of 130 nm. The sphere on the right is out of focus due to the three-dimensional nature of the sample and the limited depth of field.

described above. However, this procedure does not permit variation in the weight percent of deposited titania since loading is determined strictly by the reaction of the silanol groups with the alkoxide. Hence, a series of titania-coated silica samples was also prepared by incipient wetness impregnation to permit control of the weight loading and obtain submonolayer concentrations of titania. These preparations were also performed under flowing $N_2$ but with titanium isopropoxide (Aldrich) in toluene as precursor. The choice of precursor was purely coincidental and reflected the availability of the precursors in the two laboratories: Lehigh and New Mexico. The samples prepared by incipient wetness impregnation were dried overnight at room temperature and subsequently heated to 393 K under $N_2$ atmosphere. Final calcination was performed in $O_2$ (Linde, 99.99%) at 773 K.

The titania-coated silica was characterized by IR and Raman spectroscopies and examined in a transmission electron microscope as-prepared and after calcination at 773 and 973 K. The IR spectroscopy was performed in transmission mode by pressing the powders onto a tantalum wire mesh (Unique Wire Weaving Co., Hillside, NJ). The wire mesh was supported on a macor ceramic and stainless-steel sample mount that permitted heating the wire mesh resistively and allowed measurement of powder temperature via a chromel–alumel thermocouple spot welded to the wire mesh. The sample was contained in a 2¾-in. stainless cube that was connected to a gas handling system and to an EAI (Model 1200) mass spectrometer and pumped with a 50

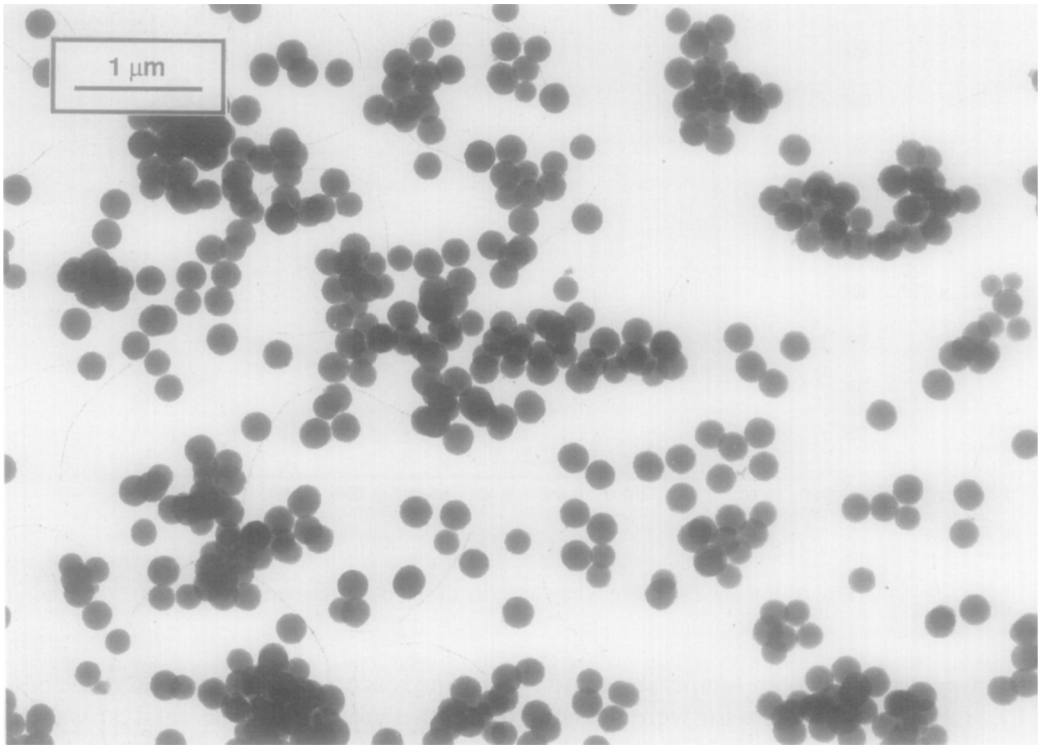


FIG. 2. Low magnification view of titania-coated silica.

liter/s Balzers turbomolecular pump. The vacuum in the sample chamber was generally $\approx 2 \times 10^{-7}$ Torr. The $CaF_2$ IR windows were mounted on $2\frac{3}{4}$-in. Conflat flanges (Harshaw part No. 8960-1C-$CaF_2$). When the sample chamber had been evacuated, the sample could be heated to 1273 K without damage to the $CaF_2$ windows, allowing us to observe the dehydroxylation and rehydroxylation of the surface.

Laser Raman spectra were obtained with the 514.5-nm line of an $Ar^+$ ion laser (Spectra Physics, Model 2020-50) operated with about 1–100 mW of power measured at the sample. The scattered radiation from the sample was directed into an OMA III (Princeton Applied Research, Model 1463) optical multichannel analyzer with a photodiode array cooled thermoelectrically to 235 K. Further details of the experimental arrangement have been described elsewhere (*4, 10, 11*). The samples were mixed with KBr powder and pressed into self-supporting discs for the Raman spectroscopy. All spectra were recorded at ambient conditions with the sample being rotated to prevent spot heating. Transmission electron micrographs were obtained on a JEOL 2000 FX microscope operated at 200 kV. The powders were supported on holey carbon films mounted on 200 mesh, 3-mm TEM copper grids. Elemental analysis was performed using a Tracor Northern 2000 EDS system using a Be window detector. The EDS spectra were analyzed using the standardless analysis program SMTF on the Tracor system using the K lines of Ti and Si.

The catalytic probe reactions used for this study were dehydration of 1-propanol and selective oxidation of methanol. The dehydration of 1-propanol was performed using 30–50 mg of sample held in a $\frac{1}{2}$-in.-o.d. quartz U-tube reactor. The reactant stream consisted of 20 sccm of He bubbled through

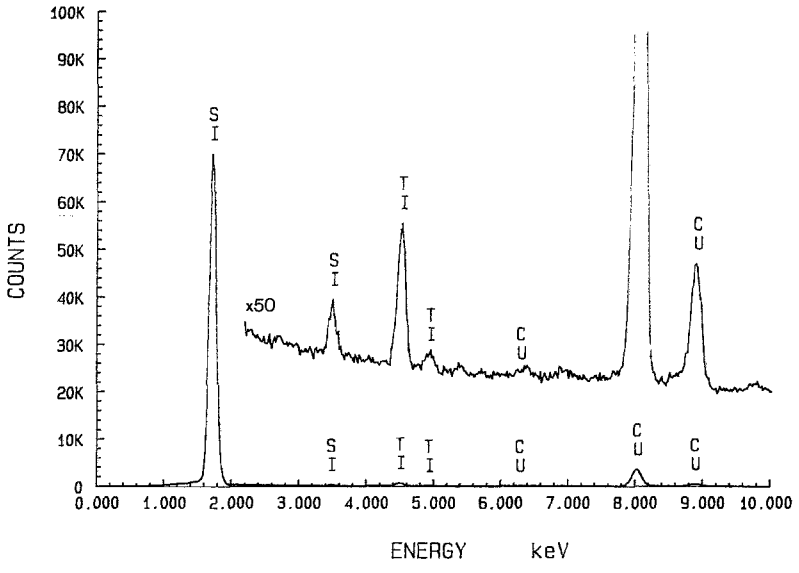


FIG. 3. Energy dispersive X-ray analysis of the titania-coated silica.

liquid 1-propanol at room temperature. All of the lines in the flow reactor were heated to prevent condensation of the 1-propanol. Reaction products were propene, dipropyl ether, and water. They were analyzed by a Varian 3400 GC using a 6-ft Porapak Q column and a thermal conductivity detector. The catalyst was activated by heating in flowing helium at 773 K overnight. After passing the reactant mixture over the catalyst for 10 min, a sample of the effluent was injected into the GC for analysis and the 1-propanol flow switched off for 20 min before the start of the next run. The rate was expressed in terms of formation of propene per unit surface area of sample per second. In this manner, reproducible activity measurements were obtained and there was no significant deactivation of the catalyst during the runs.

The methanol oxidation reaction was carried out in a downflow, isothermal, fixed-bed differential reactor operating at atmospheric pressure and a temperature of 503 K. A mixture of methanol, oxygen, and helium having a molar ratio 7 : 12 : 81 and a flow rate of 25–100 sccm was used as a reactant. Conversions were maintained at less than 5%. The reactor was vertical and made of 6-mm-o.d. Pyrex glass. The catalyst was retained in the middle of the tube using quartz wool plugs. The product stream was analyzed using an on-line gas chromatograph (HP 5840) equipped with FID and two TCDs and two packed columns.

## RESULTS AND DISCUSSION

### *Transmission Electron Microscopy*

Figure 1 shows a micrograph of a batch of silica spheres at high magnification. It can be seen from the micrograph that the powder consists of nonporous spherical particles. The silica spheres used here had an average diameter of 130 nm. Figure 2 shows the titania on silica as-prepared at low magnification. Analysis of the sample by EDS shows that the titania is present uniformly over the sample. The morphology of the silica support makes it easy to spot the presence of a second phase such as clumps of amorphous titania and very few such clumps were seen on the sample. As seen in Fig. 2, at a low magnification, the titania-coated silica spheres look very similar to the uncoated spheres suggesting that the titania has uniformly coated the surface of the sil-

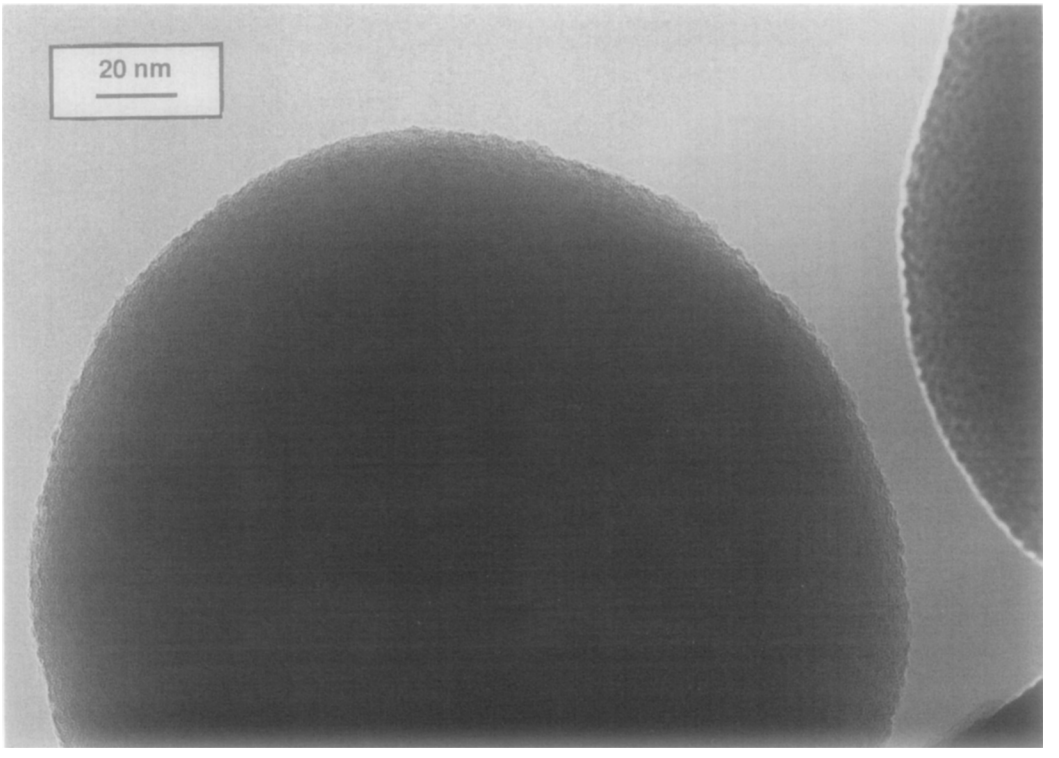


FIG. 4. High magnification view of titania-coated silica spheres. The sphere on the right is out of focus due to the three-dimensional nature of the sample.

ica. Figure 3 shows a typical EDS spectrum from this sample. The analysis of aggregates containing many silica spheres was similar to that from individual silica spheres. The average weight percent $TiO_2$ from EDS analysis on this sample was 0.6 wt%. The theoretical monolayer capacity for a 200-nm silica sphere having a geometric surface area of 12.5 $m^2/gm$ is $\approx$1.7 wt%. Figure 4 shows a higher magnification view of the titania-coated silica sample. The presence of the titania is manifested in a change in the surface texture of the silica sphere as seen from a comparison of Figs. 1 and 4. We have recently reported (*16*) similar observations concerning the reaction between the mixed metal alkoxide $((COD)Rh)_2Sn(OEt)_6$, where COD is 1,5-cyclooctadiene and hydroxylated silica spheres in which a coating of the Rh–Sn species results. It was also observed that heat treatment of the silica spheres at 773 K to reduce the surface hydroxyl concentration markedly reduced the loading of Rh–Sn on the surface of silica in the previous study (*16*). When Cabosil-fumed silica (grade HS-5) was coated with titania using a similar procedure, EDS analysis showed an average weight loading of 2.8 wt% which corresponds to $9.6 \times 10^{-5}$ $g/m^2$. Since the fumed silica charges excessively in the TEM, it is not possible to obtain images at the magnification used for Fig. 4. The low magnification images reveal no evidence for the presence of titania implying that a uniform coating has been obtained.

The titania-coated silica spheres were used as a catalyst for alcohol dehydration and Fig. 5 shows the transmission electron micrograph of the sample after the reaction measurements. The titania now appears as crystals of anatase on the surface of silica. Exposure of the titania-coated silica to alco-

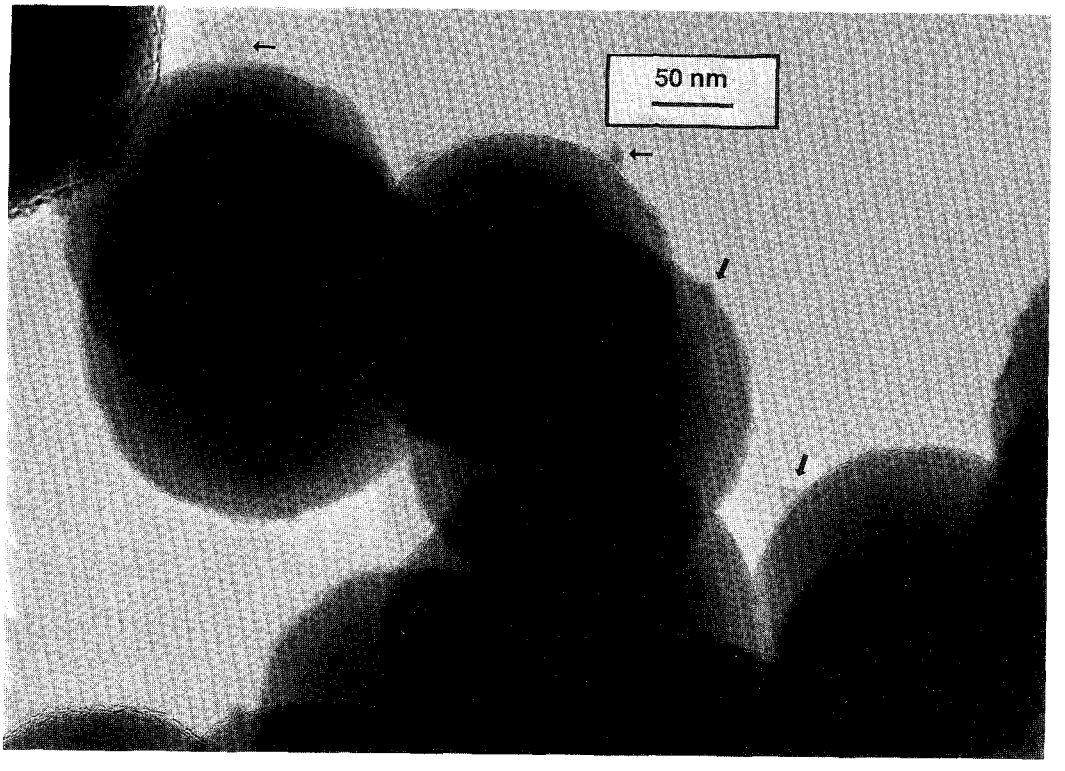


FIG. 5. Micrograph of titania-coated silica after the sample was used as a catalyst for 1-propanol dehydration. The indicated particles are crystals of anatase titania.

hol dehydration conditions appears to lead to aggregation and crystallization of the dispersed titania into crystalline anatase. The presence of water as a product of reaction of alcohol dehydration may cause cleavage of the Si–O–Ti linkages. The formation of crystals of titania may have been facilitated when the sample was treated in flowing He at 773 K overnight to clean the catalyst between runs. Figure 6 shows a micrograph of the titania-coated silica after it was used for transmission IR spectroscopy. The sample was heated at temperatures up to 1058 K in a vacuum of $1 \times 10^{-7}$ Torr to dehydroxylate the surface. It appears that the heat treatment under anhydrous conditions does not cause the titania to aggregate and crystallize into anatase crystals. Similar observations were made on another titania-coated silica sample that was used for the Raman spectroscopy measurements. In this instance, the sample was heated to 973 K in dry flowing air. Figure 7 shows a micrograph of this sample. It appears that the titania coating is not very uniform on this sample since the sphere in the center contains $\approx 1.7$ wt% $TiO_2$ while the sphere on the right contains 0.2 wt% $TiO_2$. The presence of $TiO_2$ causes a pronounced contrast that makes the sphere in the center look rougher than the sphere on the right.

*Infrared spectroscopy*

Figure 8a shows the transmission IR spectrum of silica spheres as prepared. This spectrum was obtained at a resolution of 4 $cm^{-1}$ and shows a broad feature around 3200–3700 $cm^{-1}$ which corresponds to the presence of molecular water adsorbed on the surface and hydrogen-bonded hydroxyl groups on the surface. The bands seen around 2900–3000 $cm^{-1}$ are caused by impu-

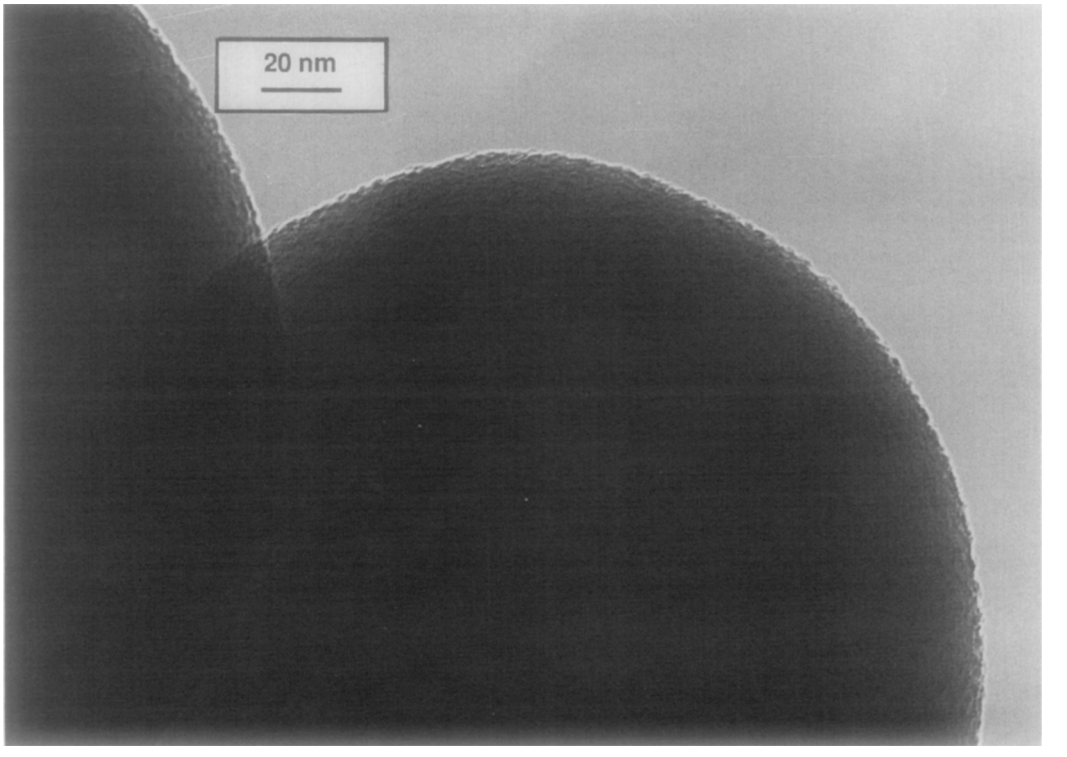


FIG. 6. Micrograph of titania-coated silica after being used for the IR spectroscopy measurements.

rities in the mirrors in the spectrometer and are always seen on this instrument. The sharp feature seen around 2300 $cm^{-1}$ is due to gas phase $CO_2$ present in the spectrometer compartment. The bands present $\approx$1800 $cm^{-1}$ and 1600 $cm^{-1}$ are due to lattice vibrations from the silica superimposed on the band due to molecular water in this air-exposed sample. The feature seen around 1400 $cm^{-1}$ may be due to the presence of carbonates. Figure 8b shows the IR spectrum of silica after heating to a temperature of 1000 K at a background pressure of $1 \times 10^{-6}$ Torr and cooling back to room temperature under vacuum. The bands due to molecular water and the carbonates have disappeared while the gas phase $CO_2$ is not seen due to a more efficient purge of the instrument. The hydroxyl region of the spectrum is now characterized by a broad band around 3500–3700 $cm^{-1}$ which represents the hydrogen-bonded hydroxyl groups on the surface. In contrast, Cabosil HS-5-fumed silica (*15*) exhibits only a sharp band at 3740 $cm^{-1}$ in the hydroxyl region of the spectrum, as seen in Fig. 9. This IR absorption band on Cabosil silica suggests the presence of only isolated hydroxyls which would imply a lower concentration of hydroxyls per square centimeters. This is consistent with the reported monolayer coverage for dispersed $V_2O_5$ per $m^2$ being 20 times lower on fumed silica than on alumina or titania (*11*).

The transmission IR spectrum of titania-coated silica spheres as-prepared looked very similar to the spectrum of uncoated silica in Fig. 8a and was characterized by a broad feature in the hydroxyl region extending from 3200 to 3700 $cm^{-1}$. Figure 10a shows the IR spectrum of titania-coated silica after heating to 1058 K and maintaining at this temperature for 10 min. The spectrum of this sample at 1058 K was markedly different from the spectrum of uncoated silica

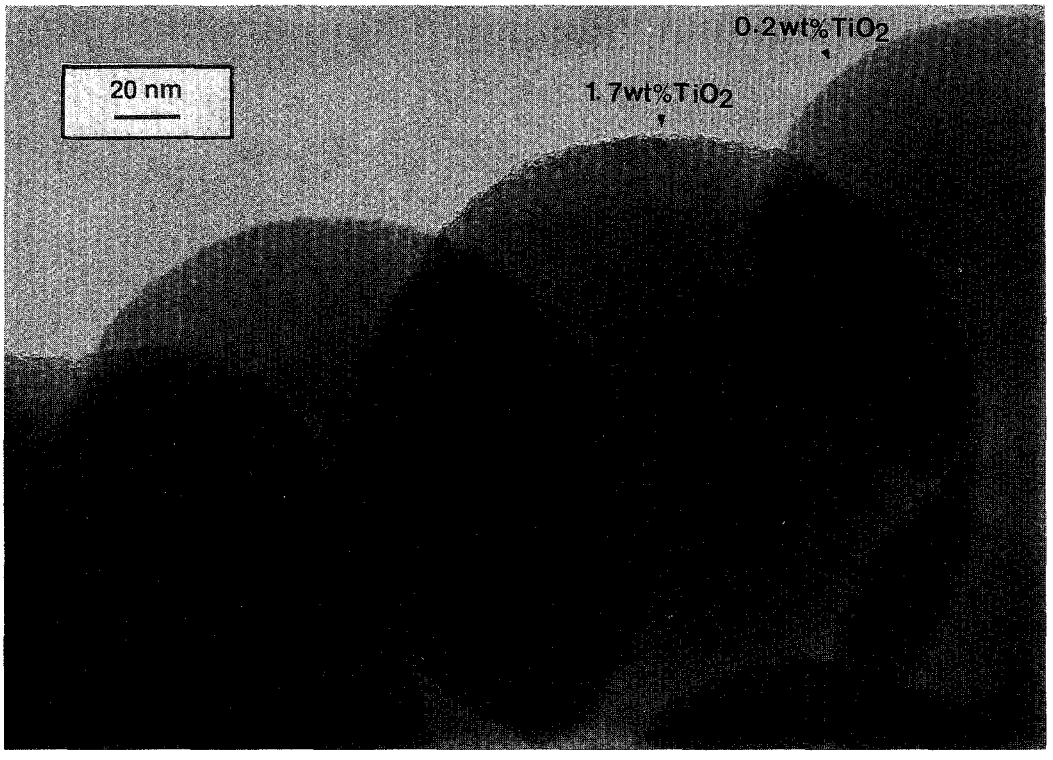


FIG. 7. Micrograph of the sample used for Raman spectroscopy measurements. This sample came from a batch different from the one described in Figs. 1–6. The sphere on the center contains ≈1.7 wt% $TiO_2$ while the one on the right has 0.2 wt% $TiO_2$. The presence of titania causes a profound increase in contrast.

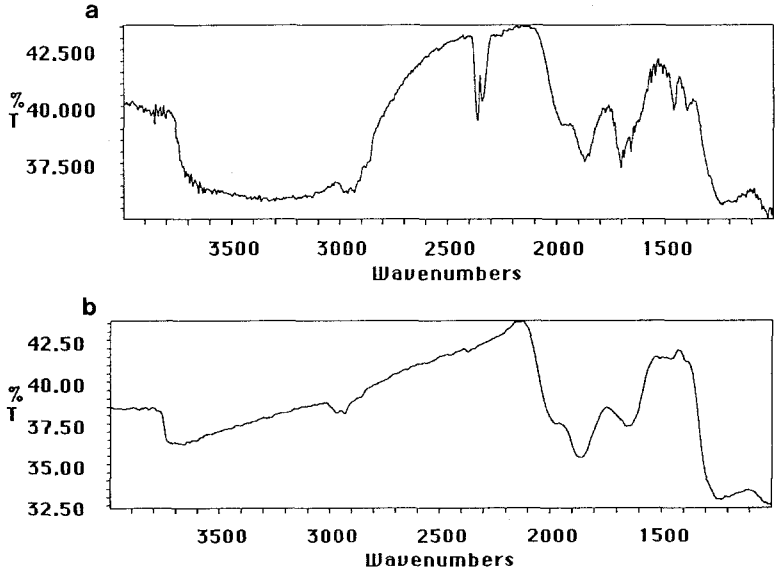


FIG. 8. Transmission IR spectrum of uncoated silica spheres (a) air exposed and (b) after heating to 1058 K at $2 \times 10^{-7}$ Torr and cooling to room temperature under vacuum.

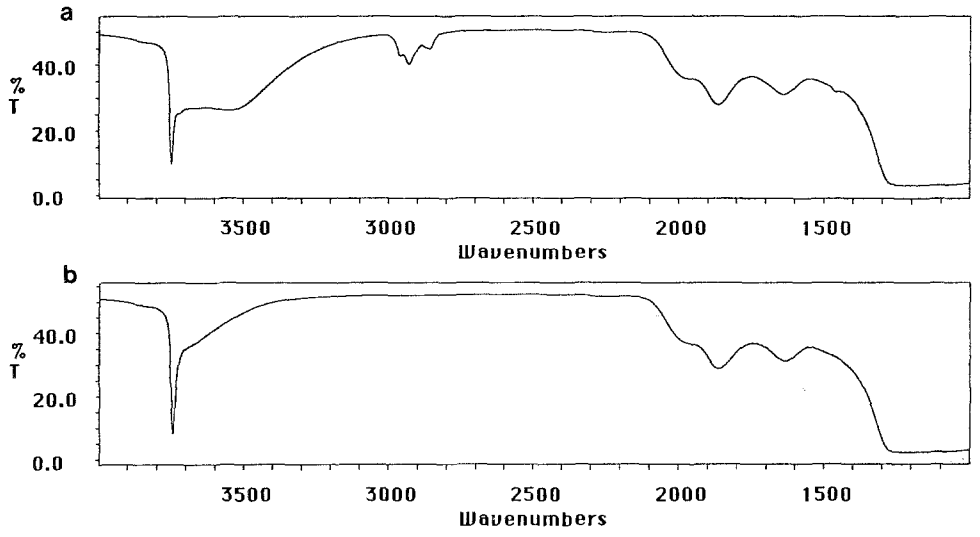


FIG. 9. Transmission IR spectrum of Cabosil HS-5 silica (a) air exposed and (b) after heating to 1023 K at 2 × $10^{-7}$ Torr and cooling to 383 K under vacuum.

spheres at this temperature. This is because the sample of titania-coated silica starts becoming opaque when heated to a temperature of around 773 K. At 1058 K, the transmittance gets so severely attenuated that it becomes impossible to distinguish any of the hydroxyl bands. Figure 10b shows the IR spectra of the titania-coated silica after

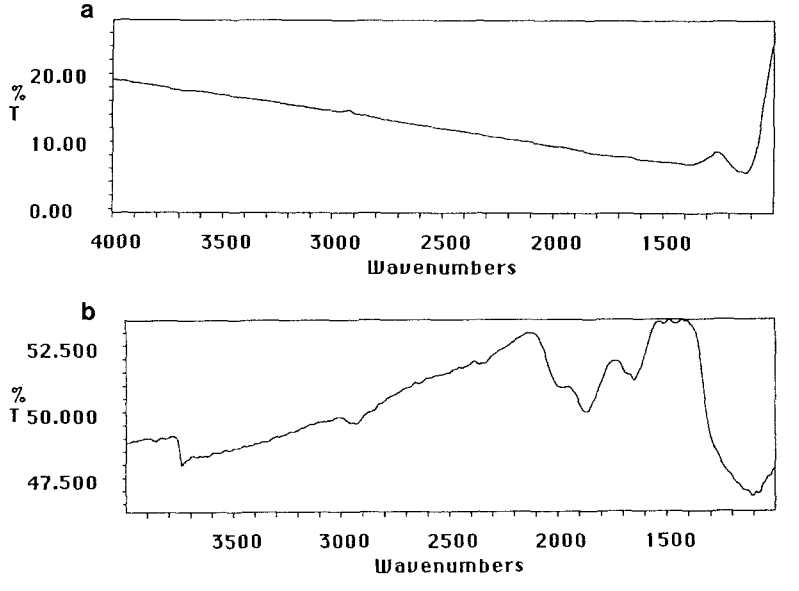


FIG. 10. Transmission IR spectrum of titania-coated silica spheres (a) heated to 1058 K at a background pressure of ≈1 × $10^{-6}$ Torr and held for 10 min and (b) after heating to 1058 K and cooling back to room temperature at a background pressure of 2 × $10^{-7}$ Torr. The spectrum acquired at 1058 K shows that the presence of titania changes the background markedly at elevated temperatures.

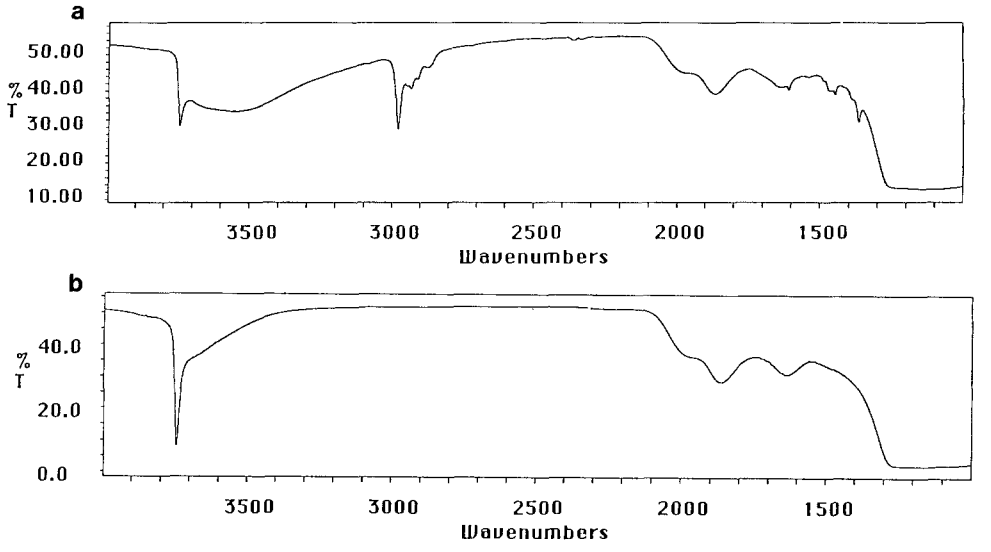


FIG. 11. Transmission IR spectrum of Cabosil HS-5 silica reacted with Ti–(O–t-$C_4H_9$)$_4$ after (a) air exposure and (b) heating to 1023 K at 2 × $10^{-7}$ Torr and cooling to room temperature.

heating to 1058 K and cooling back to room temperature in vacuum. This spectrum shows a sharp band at around 3740 $cm^{-1}$ in addition to the broad hydroxyl bands which are a characteristic feature of the silica spheres. The presence of the hydroxyl band characteristic of isolated hydroxyls suggests that the fraction of surface hydroxyls which do not hydrogen bond with neighboring hydroxyls has increased on the titania-coated silica compared to the uncoated silica spheres. Figure 11 shows the IR spectra of a sample of fumed silica containing 2.8 wt% $TiO_2$ which represents the monolayer capacity of this silica. The IR spectrum of the as-prepared sample shows a decrease in the intensity of the band due to isolated hydroxyls and an additional feature at 2960 $cm^{-1}$. This additional feature can be attributed to a C–H stretch from an aliphatic hydrocarbon, most probably the adsorbed butanol formed as a result of the reaction of the titanium alkoxide with surface silanols. After heating the sample to 1023 K and cooling to room temperature (Fig. 11b), the feature due to the adsorbed alcohol is lost and the intensity of the O–H stretch is now comparable to that on the uncoated Cabosil silica. It was found, however, that leaving the sample under vacuum for a prolonged period caused the feature at 2960 $cm^{-1}$ to reappear. We suspect this is due to the alkoxide decomposition products, namely butanol, lingering in the vacuum system and readsorbing on the silica.

*Reactivity Measurements*

The probe reaction used for characterizing the surface sites in titania-coated silica spheres was 1-propanol dehydration carried out over a temperature range of 573 to 873 K. The reactivity data is presented as an Arrhenius plot in Fig. 12 and the kinetic parameters are presented in Table 1. It is seen that silica has the lowest reactivity per square meter (BET surface area) for this reaction and titania-coated silica is intermediate between the silica and the titania. The specific reactivity of the titania-coated silica was computed assuming that the surface area of the active phase was identical to that of the silica spheres. This assump-

TABLE 1

Kinetic Parameters for the Dehydration of 1-Propanol to Propene

| Sample | Surface area ($m^2$/gm) | Preexponential factor $A$ (millimoles/s/$m^2$) | Activation energy $Ea$ (kJ/mol) |
|---|---|---|---|
| Silica spheres | 10 | $2.44 \times 10^7$ | 179 |
| 0.7 wt% Titania on silica | 10 | $1.84 \times 10^7$ | 143 |
| Degussa titania | 50 | $3.18 \times 10^7$ | 143 |

tion would be reasonable if the sample did indeed have a monolayer of titania on silica. However, the electron micrographs of the sample after reaction revealed small crystals of anatase approximately 3 nm in diameter. From the weight loading of the titania, and its particle size, we can estimate the surface area of the titania in the titania-coated silica to be 3.6 $m^2$/g of sample assuming that all of the dispersed titania had coalesced into crystals of anatase. When the data in Fig. 12 are corrected for the estimated surface area of the titania in the titania-coated silica, the specific reactivity of the titania-coated silica would actually be greater than that of the anatase titania (Degussa-P25) sample. In view of the experimental uncertainty in estimating the titania surface area in the titania coated silica, we conclude that its reactivity is comparable to that of anatase phase titania. Table 1 also shows that while the activation energy for this reaction is highest on the silica-supported catalyst, the activation energies on the titania and the titania-coated silica samples are identical within experimental error. Since the TEM data show that the titania in the titania-coated silica has aggregated into particles of crystalline $TiO_2$, we can ascribe the activity of the titania-coated silica to the crystals of anatase on the surface. Our results show that the titania-coated silica is susceptible to hydrolysis at elevated temperatures leading to phase-segregation into titania and silica.

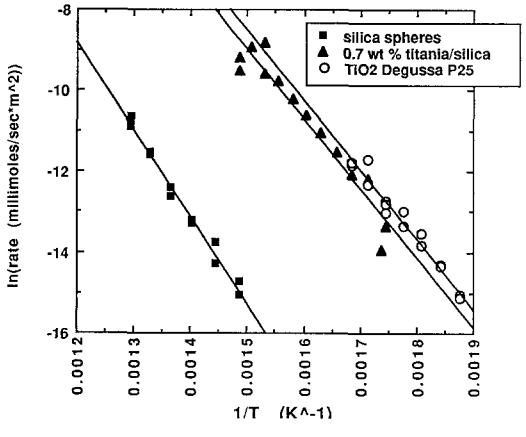


FIG. 12. Arrhenius plot for the dehydration of 1-propanol to propene.

The alcohol dehydration reactivity provides only a confirmation of the presence of titania on the surface of silica, but no evidence for any special sites created due to the dispersed oxide. Such confirmation was provided by the results of the methanol oxidation reaction. Table 2 shows the reactivity and the product distribution from this reaction. Silica is essentially inert for this reaction and not selective for methanol oxidation. However, the addition of surface titania increases the catalytic activity by two orders of magnitude and the products of selective redox reactions (formaldehyde and methylformate) are formed with a high selectivity. Crystalline titania is also active for the methanol

TABLE 2

Kinetic Parameters for Methanol Oxidation

| Catalyst | Activity × $10^4$ (mol $CH_3OH$/g cat/hr) | Selectivity (mol%) | | | |
|---|---|---|---|---|---|
| | | $CO_x$ | HCOH | MF | DME |
| $SiO_2$ Cabosil HS-5 | $7.74 \times 10^{-4}$ | 100 | | | |
| 1% $TiO_2/SiO_2$ | $7.5 \times 10^{-3}$ | 4.0 | 34 | 60 | 2.0 |
| 2% $TiO_2/SiO_2$ | $1.5 \times 10^{-2}$ | 5.0 | 33 | 60 | 2.0 |
| 4% $TiO_2/SiO_2$ | $2.3 \times 10^{-2}$ | 4.0 | 43 | 51 | 2.0 |
| $TiO_2$ Degussa P-25 | $2.3 \times 10^{-2}$ | 9.5 | | | 90.5 |

*Note.* $SiO_2$—300 $m^2/g$; $TiO_2$—50 $m^2/g$; MF, methyl formate; DME, dimethyl ether.

oxidation reaction; however, the products are not redox products but acid-catalyzed products such as dimethyl ether (DME).

*Raman Spectroscopy*

Raman spectroscopy was used to determine the nature of the dispersed titania species in the titania-coated silica samples. We found that the air-exposed samples of silica spheres as well as the titania-coated silica fluoresced excessively making it impossible to acquire good spectra. Only after heating these samples in dry air at 973 K was the fluorescence eliminated and the spectrum in Fig. 13 obtained. All samples were exposed to ambient air during the preparation of the KBr pellets for Raman spectroscopy, and the spectra were all obtained at room temperature. The Raman spectrum (Fig. 11) of the titania-coated silica imaged in Fig. 7 shows features seen also on the uncoated silica spheres and no evidence for a dispersed titania phase was seen. The absence of bands due to crystalline $TiO_2$ is in agreement with the TEM results. However, no distinguishing features due to the dispersed titania are seen, probably due to the low loading of titania on the silica spheres due to the low surface area. Figure 14 shows Raman spectra of titania dispersed on the Cabosil silica. Since it is possible to build up a higher weight loading of dispersed titania, it is easier to detect its presence. The weak features seen on the spectrum in Fig. 14 may explain why in previous studies of supported $TiO_2$ (*8, 17*) no bands due to dispersed titania could be detected. In Fig. 14, above a weight loading of 3 wt%, bands due to crystalline ($TiO_2$) anatase start to appear, suggesting that the monolayer capacity has been exceeded. In agreement with the TEM data reported above, we estimate the monolayer capacity of fumed silica to be 2.8 wt% which corresponds to $9.6 \times 10^{-5}$ g/$m^2$, only 7% of the theoretical monolayer capacity based on the BET surface area.

## SUMMARY AND CONCLUSIONS

We have shown that uniform coatings of titania on silica can be achieved by reacting Ti tert-butoxide with surface silanol groups. We believe that the titanium alkoxide reacts with the surface silanol groups with loss of alcohol to form one or more Ti–O–Si linkages which are stable in a dry atmosphere. The bound titanium oxo-alkoxide may undergo further hydrolysis and condensation on exposure to moist air to yield a hydrous oxide. On 200-nm silica spheres having a geometric surface area of ≈12.5 $m^2$/gm, we would expect a monolayer loading ≈1.7 wt%. Hence, the observed weight loadings of titania on silica seen in this study, approximately 0.6–1.7 wt%, are consistent with the presence of up to a monolayer of titania. In other experiments, we have observed that if the silica spheres are not dried before coat-

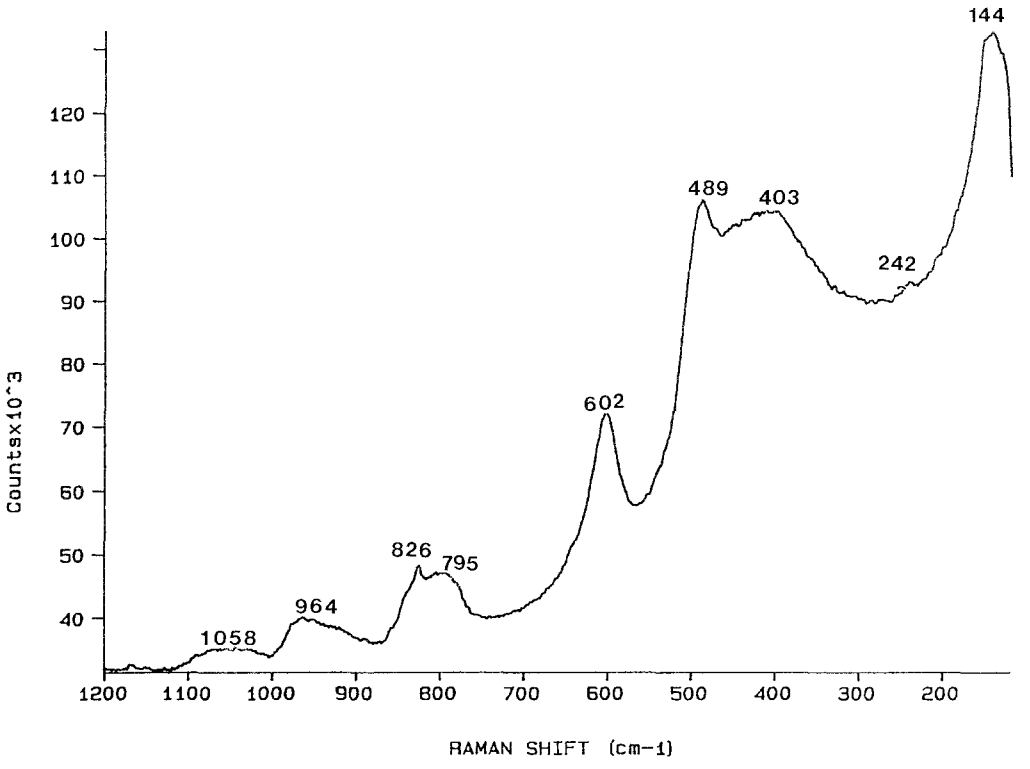


FIG. 13. Raman spectrum of titania-coated silica spheres after heating in dry air at 973 K. This is the same sample imaged in Fig. 7.

ing, weight loadings greater than the monolayer capacity of silica can be obtained but these samples always contain observable particles of crystalline $TiO_2$ on the silica surface. On the other hand, when the titania is present as a dispersed phase, the only observable feature by TEM is an increase in contrast apparent as a surface texturing of the silica. Hence, the use of nonporous oxide spheres as a substrate permits the use of TEM to detect very sensitively the presence of monolayers of a second oxide phase.

The surface concentration of dispersed titania on Cabosil silica (approximately $9.6 \times 10^{-5}$ g/m$^2$) is only 7% of the theoretical monolayer capacity ($1.37 \times 10^{-3}$ g/m$^2$). The IR spectrum of Cabosil silica is consistent with the presence of isolated hydroxyl groups. It appears that the surface of fumed silica lacks the surface hydroxyl density that would lead to significant hydrogen bonding between neighboring hydroxyls. In this regard, fumed silica is very different from other oxides such as $Al_2O_3$, MgO, and $TiO_2$. On the other hand, the Stober spheres prepared by base-catalyzed condensation of tetraethylorthosilicate show evidence for considerable hydrogen bonding with neighboring hydroxyls, and the observed monolayer capacity of these spheres is close to that expected theoretically based on the packing of titania in the (101) plane of anatase. These results would suggest that multiple binding sites from neighboring hydroxyls, such as those available on the Stober spheres, may be required to support the dispersed titania.

This study has also shown that dispersed titania on silica is stable in dry air at temperatures up to 1058 K and no formation of crystalline $TiO_2$ was seen under these conditions. The dispersed titania does not, how-

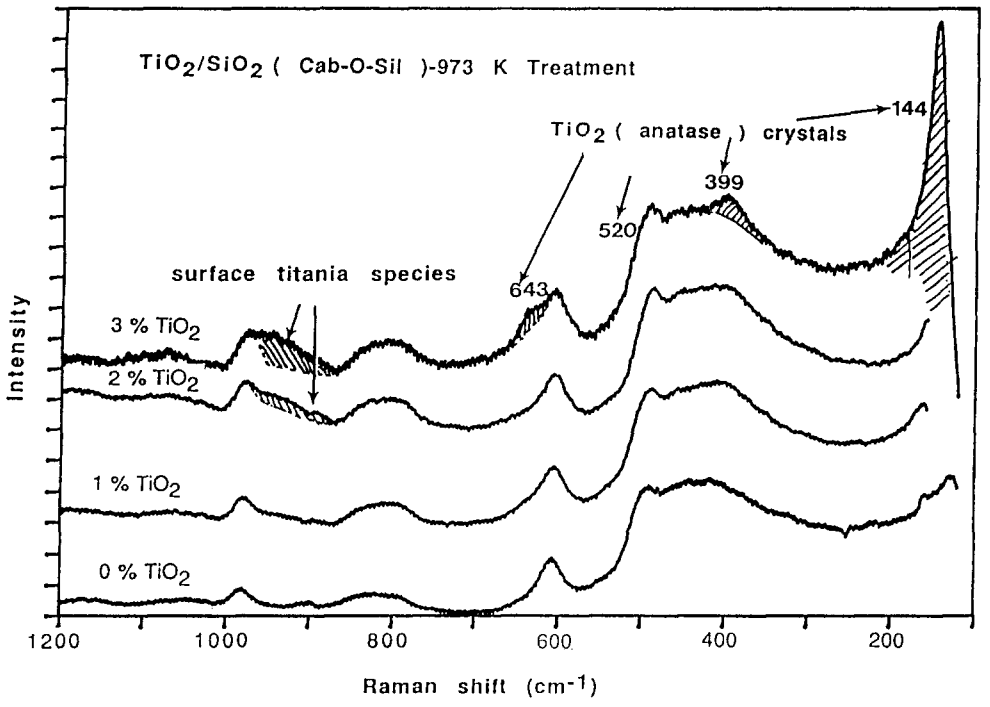


FIG. 14. Raman spectra of Cabosil HS-5 silica having 0–3 wt% $TiO_2$. The samples were heated in dry air at 973 K. Weak features suspected to be due to dispersed titania are visible on the 2 and 3 wt% samples while crystalline $TiO_2$ (anatase) is first evident on the 3 wt% sample.

ever, appear to be stable during heat treatments in the presence of water vapor. For instance, during the alcohol dehydration experiments, the titania appeared to migrate over the surface and form faceted crystals of anatase ≈3 nm in diameter as seen in Fig. 5. The presence of titania in these titania-coated silica was also detected using 1-propanol dehydration as a test reaction. Since titania is approximately $8.5 \times 10^2$ times more reactive than the silica surface (as seen from Fig. 10), the presence of a titania coating causes a dramatic increase in the alcohol dehydration activity. The titania-coated silica spheres were approximately $6.6 \times 10^2$ times more reactive than uncoated silica at 673 K, assuming no change in surface area. We can ascribe this reactivity to the presence of crystalline titania particles on the silica surface as seen after reaction by TEM (Fig. 5). The presence of dispersed titania on the silica surface is further confirmed by the formation of selective oxidation products from methanol, not seen either on the uncoated silica or on pure crystalline titania.

## ACKNOWLEDGMENTS

Financial support for this research from NSF grant CTS 89-12366 is gratefully acknowledged. The IR spectrometer used in this work was acquired through NSF equipment grant CTS 89-06023. Electron microscopy was performed at the microbeam analysis facility within the Department of Geology at the University of New Mexico. We thank Katherine Blankenburg for experimental assistance. Sandia National Laboratory is supported by U.S. Department of Energy Grant DE-AC04-76DP00789.

## REFERENCES

1. Kung, H. H., *Stud. Surf. Sci. Catal.* **45** (1989).
2. Baiker, A., Dollenmeier, P., Glinski, M., and Reller, A., *Appl. Catal.* **35,** 351 (1987).
3. Murrell, L. L., *J. Catal.* **79,** 203 (1983).
4. Hardcastle, F. D., and Wachs, I. E., *J. Raman Spectrosc.* **21,** 683 (1990).
5. Iwasawa, Y., *in* "Proceedings of the International Symposium on Acid–Base Catalysis" (K. Tanabe and H. Hattori, Eds.), p. 267. VCH, New York, 1989.

6. Oyama, S. T., Went, G. T., Lewis, K. B., Bell, A. T., and Somorjai, G. A., *J. Phys. Chem.* **93,** 6786 (1989).
7. Gai, P. L., Goringe, M. J., and Barry, J. C., *J. Microsc.* **142,** 9 (1986).
8. Reichmann, M. G., and Bell, A. T., *Langmuir* **3,** 111 (1987).
9. Sattler, M. L., and O'Keefe, M. A., *in* "Proceedings, 45th Annual Meeting Electron Microscopy Society of America" (G. W. Bailey, Ed.), p. 104. San Francisco Press, 1987.
10. Hardcastle, F. D., and Wachs, I. E., *in* "Proceedings, 9th International Congress on Catalysis, Calgary, 1988" (M. J. Phillips and M. Ternan, Eds.), p. 1449. The Chemical Institute of Canada, Ottawa, 1988.
11. Wachs, I. E., *Chem. Eng. Sci.* **45,** 2561 (1990).
12. McDaniel, M. P., Welch, M. B., and Dreiling, *J. Catal.* **82,** 118 (1983).
13. Vogt, E. T. C., Boot, A., van Dillen, A. J., Geus, J. W., Janssen, F. J. J. G., and van den Kerkhof, F. M. G., *J. Catal.* **114,** 313 (1988).
14. Stober, W., Fink, A., and Bohn, E., *J. Colloid Interface Sci.* **26,** 62 (1968).
15. Cabot Corporation, "Cab-O-Sil Properties and Functions," Technical brochure, 1985.
16. Anderson, S., Datye, A. K., Wark, T. A., and Smith, M. H., *in* "Materials Research Society Extended Abstracts," Vol. EA-24, p. 111, 1990; *Catal. Lett.*, **8,** 345 (1991).
17. Stranick, M., Houalla, M., and Hercules, D. M., *J. Catal.* **106,** 362 (1987).